served in $\bar{p}$-p kaonic annihilations at 3.7 BeV/c, has decreased with the increased initial-state energy. The production of $K^*(890)$ has dropped from the 50% level at 3.7 BeV/c to ~10% at 7 BeV/c among the final states examined. Neither ρ nor ω has been observed among the two-vee events at 7 BeV/c, although there is some evidence for the formation of $K^*(1400)$.

A study of the energy dependence of the fraction of annihilation events leading to kaons and pions in the final state indicates that after an initial rise (from ~4%) for antiproton capture at rest, the kaonic annihilations reach ~10% of the total annihilation cross section and remain fairly constant up to 7 BeV/c, where the fraction is (10.2±3.1)%. This is inconsistent with the predictions of the statistical theory.

Our data at 7 BeV/c show a $K_1^0K_1^0$ enhancement near threshold similar to the effect observed at 3.7 BeV/c. There is also a $K_1^0K_1^0$ enhancement at 1140 MeV, but no conclusive statement can be made concerning the significance of this effect because of the limited statistics. It is interesting, however, that a similar effect exists in the 3.7-BeV/c data.

ACKNOWLEDGMENTS

We wish to acknowledge the cooperation of the AGS personnel, the bubble-chamber crew and our scanners and measurers for their cooperation during the various phases of this work. Those of us from Yale University would like to thank Dr. R. P. Shutt for his hospitality during our stay at Brookhaven National Laboratory for the experimental run. Professor C. Baltay and Professor T. Ferbel participated in the early stages of this study, and their help is gratefully acknowledged. We wish to thank the computer centers at Yale University, Brookhaven National Laboratory, and New York University for their cooperation and assistance during the course of this experiment.

PHYSICAL REVIEW VOLUME 158, NUMBER 5 25 JUNE 1967

Reaction $K^+p \to K^+p\pi^+\pi^-$ at 2.26 BeV/c*

FREDERICK BOMSE, SAMUEL BORENSTEIN, JAMES COLE, DANIEL GILLESPIE, ROBERT KRAEMER, GEORGE LUSTE, IRVIN MILLER, EDWARD MOSES, AIHUD PEVSNER, RANDHIR SINGH, AND RICHARD ZDANIS

Department of Physics, The Johns Hopkins University, Baltimore, Maryland

(Received 7 November 1966)

The reaction $K^+p \to K^+p\pi^+\pi^-$ at 2.26 BeV/c is investigated. It is found to be dominated by the simultaneous production of the K^* (895 MeV) and N^* (1238 MeV) resonances. The production and decay angular distributions of these resonances in the double-resonance channel are analyzed and the results compared with the predictions of a single-particle-exchange model. These distributions are consistent with the assumption that the primary production mechanism responsible for the reaction $K^+p \to K^{*0}N^{*++} \to K^+\pi^-\pi^+p$ at 2.26 BeV/c is the exchange of a single π meson. A search is conducted in this channel for other possible resonant states. A Monte Carlo analysis is utilized for this purpose. The data are not found to be consistent with the production of any other resonances except the aforementioned K^* (895 MeV)and N^* (1238 MeV).

1. INTRODUCTION

WE have investigated the reaction $K^+p \to K^+p\pi^+\pi^-$ in the 20-in. hydrogen bubble chamber at Brookhaven National Laboratory. In our exposure, the K^+ beam had a laboratory momentum at the chamber entrance window of 2.260 BeV/c with a full width at half-maximum of 0.045 BeV/c.

We find this reaction to be highly resonant and dominated by the simultaneous production of the K^* (895 MeV) and N^*(1238 MeV). In addition, there is evidence for the production of these resonances singly via the channels $K^+p \to K^{*0}p\pi^+$ and $K^+p \to N^{*++}K^+\pi^-$.[1]

We have analyzed the production and decay angular distributions of the K^* and N^* in the double-resonance channel and compared our results with theoretical predictions of a single-particle-exchange model.[2–6] These experimental distributions are consistent with the assumption that the primary production mechanism responsible for the reaction $K^+p \to K^{*0}N^{*++} \to K^+\pi^-\pi^+p$ is the exchange of a single π meson between the incoming particles.

We have also conducted an extensive search for other possible resonant states which could be observed in the

* Supported in part by the National Science Foundation, the Air Force Office of Scientific Research Grant No. AF AFOSR 234-65, and the U. S. Atomic Energy Commission Computation Center.

[1] A preliminary report on this work was made at the 1963 Athens Conference on Resonant Particles.

[2] J. D. Jackson, Nuovo Cimento **34**, 1644 (1964).

[3] K. Gottfried and J. D. Jackson, Nuovo Cimento **33**, 309 (1964).

[4] K. Gottfried and J. D. Jackson, Nuovo Cimento **34**, 735 (1964).

[5] J. D. Jackson, Rev. Mod. Phys. **37**, 484 (1965).

[6] J. D. Jackson, J. T. Donahue, K. Gottfried, R. Keyser, and B. E. Y. Svennson, Phys. Rev. **139**, B428 (1965).

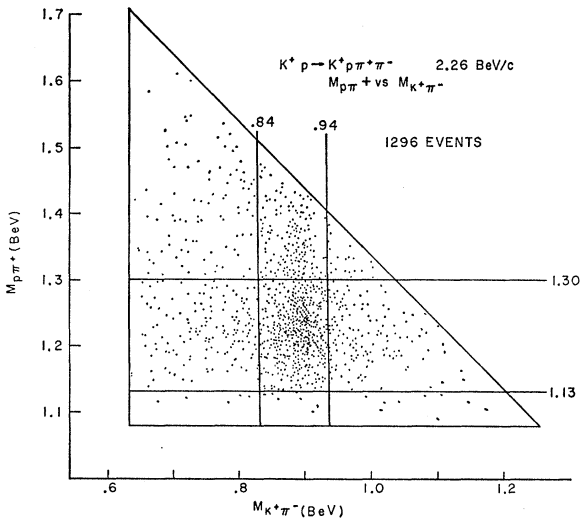

FIG. 1. Effective $K^+\pi^-$ mass versus effective $p\pi^+$ mass.

reaction $K^+p \to K^+p\pi^+\pi^-$. To this end, we assumed that only amplitudes relating to $K^*(895)$ and $N^*(1238)$ production (as well as phase space) occurred in the reaction and generated a series of Monte Carlo events based on this assumption. When all possible mass spectra obtained from the Monte Carlo events were compared with those of the experiment, no significant differences were observed. We therefore concluded that our data were not consistent with the production of any resonant state other than the $K^*(895)$ and the $N^*(1238)$.

2. EXPERIMENTAL METHOD

Approximately 100 000 bubble chamber photographs yielded 4711 four-prong events. After measurement,

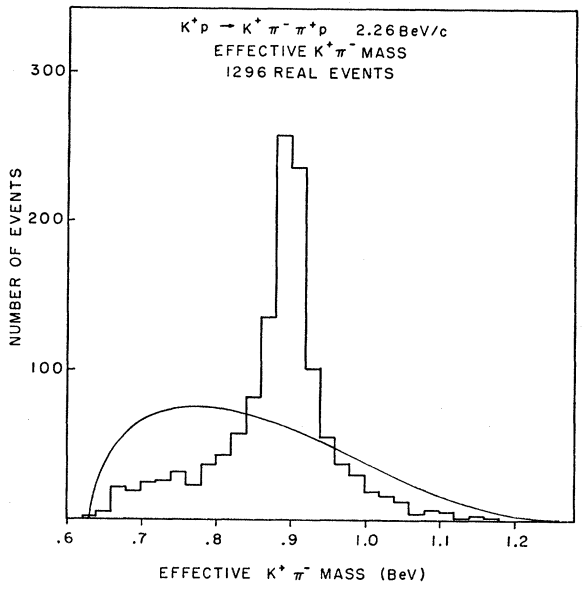

FIG. 2. Number of events versus effective $K^+\pi^-$ mass.

stereo reconstruction, kinematic fitting, and ionization checking, 1296 of these were positively identified as belonging to the reaction $K^+p \to K^+p\pi^+\pi^-$. A more detailed description of the data reduction process is presented in Ref. 7.

3. CROSS SECTIONS

We determine the cross section of the reaction $K^+p \to K^+p\pi^+\pi^-$ at 2.26 BeV/c from the total K^+ beam length and number of reactions observed within a specified fiducial volume. We utilize a subsample of 30 000 frames, all of which were scanned twice. We estimate the purity of the K^+ beam from the number of τ and τ-like decays counted in this sample of the film. The procedure is discussed more fully in Ref. 7, and yields a beam purity of $(80\pm3)\%K^+$. The number of reactions is corrected for the over-all scanning efficiency, which is 97%, as determined from the two independent scans. A total K^+ beam length of 12.95×10^6 cm and 811 reactions of the type $K^+p \to K^+p\pi^+\pi^-$ give a total cross section:

$$\sigma(K^+p \to K^+p\pi^+\pi^-) = 1.7\pm0.2 \text{ mb}.$$

We estimate (using a method to be described later) that the double-resonance process $K^+p \to K^{*0}N^{*++}$ accounts for 48% of all events of the type $K^+p \to K^+p\pi^+\pi^-$. This yields a partial cross section

$$\sigma(K^+p \to K^*N^* \to K^+p\pi^+\pi^-) = 0.8\pm0.1.$$

These results are compared with those of other experiments at different energies in Table I.

TABLE I. Cross section for the reaction $K^+p \to K^+p\pi^+\pi^-$.

Incoming K^+ lab momentum (BeV/c)	$\sigma(K^+p \to K^+p\pi^+\pi^-)$	Reference
1.96	1.7±0.2	a
2.26	1.7±0.2	Present experiment
2.97	2.3±0.3	b
	$\sigma(K^+p \to K^{*0}N^{*++} \to K^+p\pi^+\pi^-)$	
1.96		
2.26	0.8±0.1	Present experiment
2.97	1.2±0.2	b

[a] G. Goldhaber, W. Chinowsky, S. Goldhaber, W. Lee, and T. O'Halloran, Phys. Letters 6, 62 (1963).
[b] Reference 8.

4. K^* AND N^* DISTRIBUTIONS

In Fig. 1 we present a kinematic scatter plot for all events fitting the hypothesis $K^+p \to K^+p\pi^+\pi^-$. The effective $K^+\pi^-$ mass is plotted along the horizontal axis and the effective $p\pi^+$ mass along the vertical axis. The strong enhancement in the region 840 MeV$\leqslant M_{K^+\pi^-} \leqslant$940 MeV and 1130 MeV$\leqslant M_{p\pi^+} \leqslant$1300 MeV is evident. In Figs. 2 and 3 we plot the projections of the

[7] F. Bomse, S. Borenstein, J. Cole, D. Gillespie, G. Luste, E. Moses, A. Pevsner, and R. Zdanis (to be published).

kinematic triangle plot on the $M_{K^+\pi^-}$ and $M_{p\pi^+}$ axes, respectively. The solid curves are appropriate Lorentz-invariant phase spaces normalized to the total number of events. We return to these plots later.

Figure 4 shows the production angular distribution for the K^* system in the over-all center-of-mass system for the double-resonance events. The strong forward peaking of this distribution is taken as evidence that the reaction may be mediated by a peripheral or single-particle exchange mechanism. We analyze the decay correlations and production differential cross sections accordingly.

The decay angular distributions are observed in a coordinate system defined in the rest frame of the resonance in question. The z axis of this system lies along the direction of the incoming particle, the y axis along the production plane normal and the x axis along the direction of the cross product of y with z. The general form of the K^* and N^* angular distributions that account for conservation of angular momentum and parity

TABLE II. Experimental K^* and N^* density matrices corresponding to K^*-N^* production in the reaction $K^+p \to K^{*0}N^{*++} \to K^+\pi^-\pi^+p$.

Element	K^* density matrix Value at 2.26 BeV/c	Value at 3.0 BeV/c[a]
ρ_{00}	0.56±0.03	0.76±0.05
ρ_{1-1}	−0.004±0.03	−0.03±0.03
$\mathrm{Re}\rho_{10}$	−0.09 ±0.02	−0.13±0.02
Element	N^* density matrix Value at 2.26 BeV/c	Value at 3.0 BeV/c[a]
ρ_{33}	0.19 ±0.03	0.01 ±0.04
$\mathrm{Re}\rho_{31}$	−0.05 ±0.02	0.07 ±0.02
$\mathrm{Re}\rho_{3-1}$	0.0005±0.02	−0.035±0.035

[a] Reference 8.

are well known.[2–6] They are:

$$W_{K^*}(\cos\theta,\phi) = (3/4\pi)[\rho_{00}\cos^2\theta + \tfrac{1}{2}(1-\rho_{00})\sin^2\theta - \rho_{1-1}\sin^2\theta\cos 2\phi - \sqrt{2}\,\mathrm{Re}\rho_{10}\sin 2\theta\cos\phi], \quad (1)$$

$$W_{N^*}(\cos\theta,\phi) = (3/4\pi)[\rho_{33}\sin^2\theta + (\tfrac{1}{2}-\rho_{33})(\tfrac{1}{3}+\cos^2\theta) - 2/\sqrt{3}\,\mathrm{Re}\rho_{31}\sin 2\theta\cos\phi - 2/\sqrt{3}\,\mathrm{Re}\rho_{3-1}\sin^2\theta\cos 2\phi], \quad (2)$$

where (θ,ϕ) are spherical polar angles defined in the coordinate system described above, and W_{N^*}, W_{K^*} are normalized to unity over a sphere. The experimental values of the ρ_{ij}, the density matrix elements of the resonances may shed some light on the nature of the exchanged particles. We determine the K^* and N^* density matrix elements for the double-resonance events exactly from the data as described in Ref. 7. We remark here that a double-resonance event is one for which the effective $K^+\pi^-$ and $p\pi^+$ masses satisfy 840 MeV $\leqslant M_{K^+\pi^-} \leqslant$ 940 MeV and 1130 MeV $\leqslant M_{p\pi^+} \leqslant$ 1300 MeV. The results are shown in Table II.

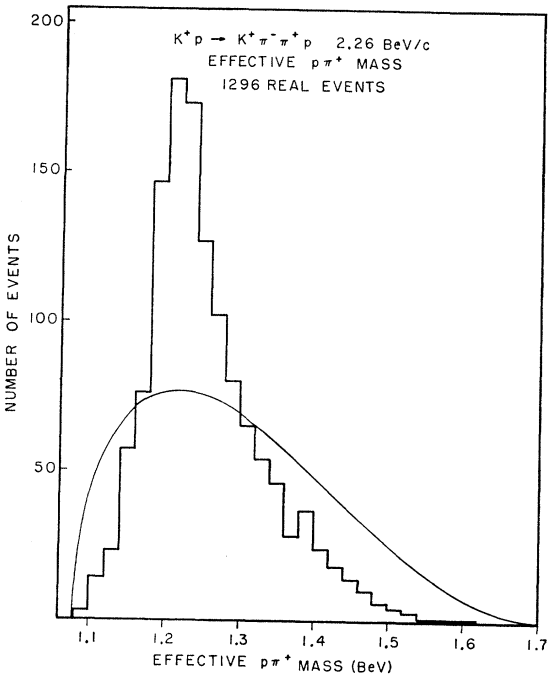

FIG. 3. Number of events versus effective $p\pi^+$ mass.

We recall[7] that for the K^* decay, a value of ρ_{00} near zero indicates predominantly vector meson exchange and a $\sin^2\theta$ angular distribution, while a larger value of this parameter indicates pseudoscalar meson exchange and a predominantly $\cos^2\theta$ angular distribution. The

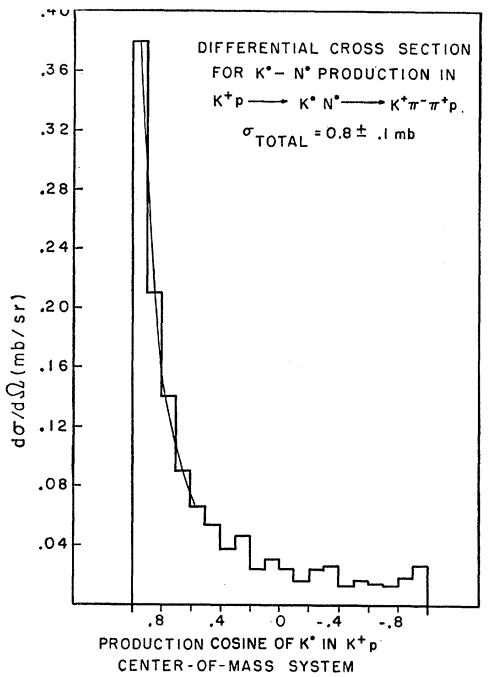

FIG. 4. Differential cross section for double-resonance production ($K^+p \to K^*N^*$) versus center-of-mass production cosine of K^*.

element ρ_{1-1} is a measure of the departure of the Treiman-Yang or ϕ angular distribution from isotropy. It is expected to be very small for pseudoscalar meson exchange and to produce a Treiman-Yang distribution which is isotropic. Our value of 0.56 ± 0.03 for ρ_{00} produces after integration over ϕ a distribution $W_{K^*}(\cos\theta) = 1+(1.5\pm0.3)\cos^2\theta$. This is shown, normalized to the total number of events in Fig. 5. Furthermore, our value of ρ_{1-1} of -0.004 ± 0.03 gives a fitted Treiman-Yang distribution of $W_{K^*}(\phi)=1-(0.02\pm0.11)\sin^2\theta$. This nearly isotropic curve is shown normalized to the total number of events in Fig. 6. The off-diagonal element $\mathrm{Re}\rho_{10}$ is -0.09 ± 0.02 and is not consistent with zero. This may indicate that absorptive effects due to competing channels are important. The K^* decay angular distributions allow us to conclude that the production mechanism of the reaction $K^+p \to K^{*0}N^{*++}$ is consistent with the exchange of a psuedoscalar meson.

To check this we consider the experimental values of the N^* density matrix elements. The result obtained for ρ_{33} is 0.19 ± 0.03 and leads to a $\cos\theta$ distribution of $W_{N^*}(\cos\theta)=1+(0.4\pm0.2)\cos^2\theta$. We present this curve normalized to the total number of events in Fig. 7. We remark that the experimental N^* decay distribution in $\cos\theta$ (histogram in Fig. 7) shows a marked forward-backward asymmetry. On the high side from $\cos\theta=0$ to $\cos\theta=1$ it rises more or less as $\cos^2\theta$, while on the low side from $\cos\theta=-1$ to $\cos\theta=0$ it is nearly flat. We note that for pseudoscalar exchange ρ_{33} is expected to be near zero and the distribution, approximately $(1+3\cos^2\theta)$. The high value of ρ_{33} is a reflection of this asymmetry. A possible explanation for this asymmetry is that final-state interactions may be important for the wide ($\sim$100 MeV) N^*. Figure 8 shows the experimental

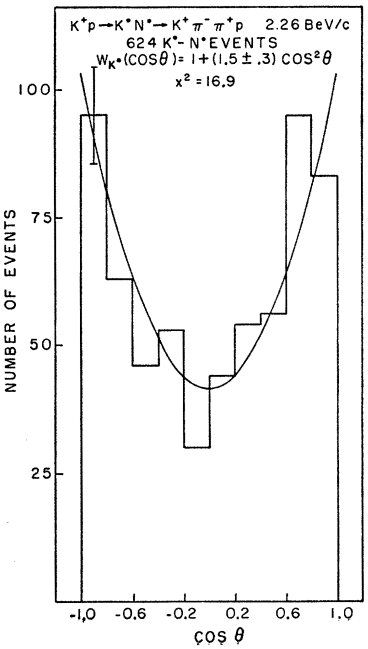

FIG. 5. $\cos\theta$ distribution of K^* from $K^+p \to K^*N^*$.

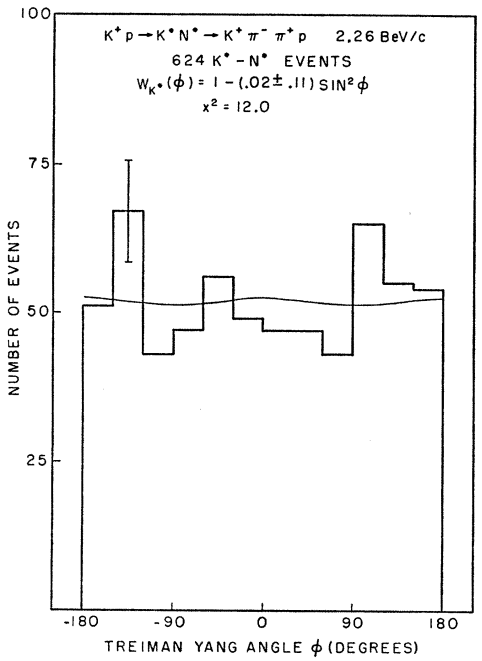

FIG. 6. Treiman-Yang or ϕ distribution of K^* from $K^+p \to K^*N^*$.

Treiman-Yang distribution for the N^*. The parameter $\mathrm{Re}\rho_{3-1}$ is 0.0005 ± 0.02 and the corresponding fitted curve is $W_{N^*}(\phi)=1+(0.002\pm0.09)\sin^2\phi$ which is very nearly isotropic. For pseudoscalar exchange this is expected to be the case. We compare the K^* and N^* density matrices determined in this experiment with those of the CERN group[8] in Table II.

We now return to the K^* production angular distribution in Fig. 4. The solid curve is the theoretical prediction of the single-pion-exchange model with absorptive effects included[6] for the reaction $K^+p \to K^{*0}N^{*++} \to K^+p\pi^+\pi^-$, normalized to our experimental differential cross section at $\cos\theta_{K^*}=0.95$. The absolute cross section is far too large. We have performed the indicated normalization to see how well the shape of our cross section agrees with the theory. As can be verified from Fig. 4, the agreement of the shapes is excellent. The theoretical curve was generated by Dr. J. D. Jackson and coworkers at The University of Illinois.

5. THE MONTE CARLO TECHNIQUE

We pointed out above that the reaction $K^+p \to K^+p\pi^+\pi^-$ at 2.26 BeV/c is dominated by the simultaneous production of the K^*(895 MeV) and N^*(1238 MeV) resonances. These appear respectively as strong peaks above the predictions of ordinary phase space in the $K^+\pi^-$ and $p\pi^+$ mass spectra. We now consider the effects of this resonance production on the other mass spectra

[8] M. Ferro-Luzzi, R. George, Y. Goldschmidt-Clermont, V. P. Henri, B. Jongejans, D. W. G. Leith, G. R. Lynch, F. Muller, and J.-M Perreau, Nuovo Cimento 39, 417 (1965).

in this channel. In particular we wish to determine if various enhancements above phase space are merely kinematic reflections of the strong K^*-N^* production or if they represent real physical states in their own right. To this end we have developed a Monte Carlo technique.

In applying this technique we first make a reasonable guess as to all the processes that are operative in the reaction $K^+p \to K^+p\pi^+\pi^-$ at our energy. This complete set of assumed processes constitutes a model for the reaction. In our model we assume an incoherent mixture of the following four processes: (a) a process with no correlations whatever among any of the particles, that is, a process described by a constant matrix element; (b) a double-resonance process with simultaneous correlations between the K^+ and π^- and the proton and π^+; (c) a single-resonance process with a correlation between the K^+ and π^- mesons only; (d) another single-resonance process with a correlation between the proton and π^+ meson only.

Processes (a) through (d) may be described in a short-hand notation as follows:

(a) $K^+p \to K^+p\pi^+\pi^-$;

(b) $K^+p \to K^*N^* \to K^+p\pi^+\pi^-$;

(c) $K^+p \to K^*p\pi^+ \to K^+p\pi^+\pi^-$;

(d) $K^+p \to K^+\pi^-N^* \to K^+p\pi^+\pi^-$.

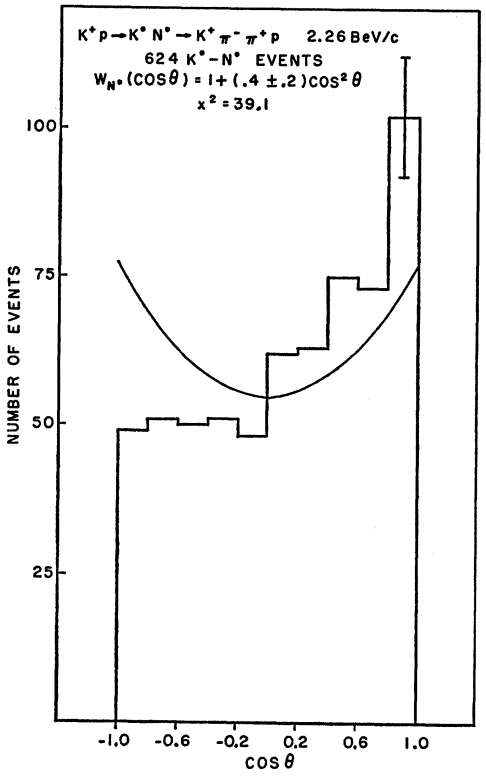

FIG. 7. Cosθ distribution of N^* from $K^+p \to K^*N^*$.

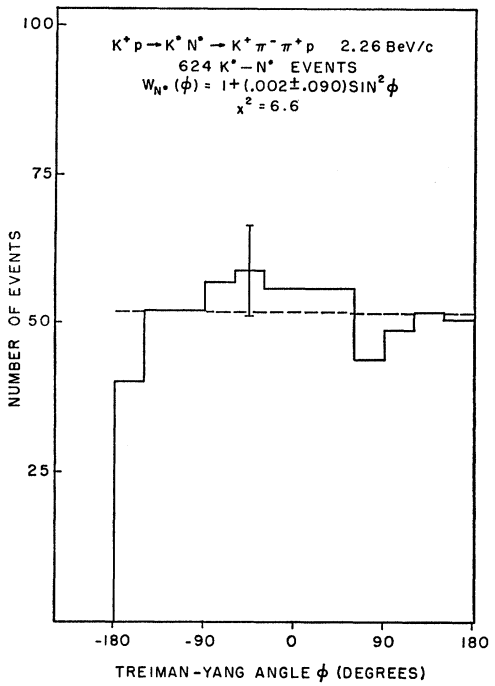

FIG. 8. Treiman-Yang or ϕ distribution of N^* from $K^+p \to K^*N^*$.

We do not write down theoretical amplitudes corresponding to these processes but attempt to get information about them from the experimental data through the $K^+\pi^-$ and $p\pi^+$ mass distributions and the angular distributions of the K^* and N^* events. We use this information to generate a set of fictitious events which are constructed so as to reproduce the various distributions (mass spectra and angular distributions) of the assumed model, that is, to reproduce processes (a) through (d) above. Using these fictitious events we then plot all the mass spectra that can be formed from the final-state particles and compare these one by one with the corresponding experimental spectra. If there is agreement between the real and fictitious mass spectra, then we may say that the proposed model is consistent with the data. Lack of agreement between the two sets of spectra is an indication that some process was not included in the model. For example, an enhancement in some mass distribution above phase space, in the experimental events which is not duplicated in the fictitious events is evidence that the enhancement may be a real effect and not a reflection of K^* or N^* production.

Our Monte Carlo calculation was done on an IBM 7094 computer using a program developed at Johns Hopkins called SIMULATE. We now proceed to describe the main features of operation of this program. It is capable of generating events with any number of final-state particles but we will only discuss the four-particle state here. We will also key the discussion to our reaction $K^+p \to K^+p\pi^+\pi^-$ and make use of our assumed model for this reaction.

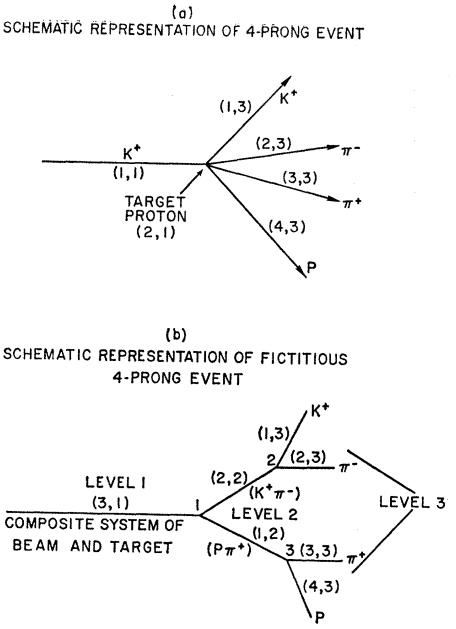

FIG. 9. Schematic representation of 4-prong event according to SIMULATE.

SIMULATE operates by breaking events down into a series of two-body vertices. Figure 9 is a schematic representation of a simulated event of the type $K^+p \rightarrow K^+p\pi^+\pi^-$. The upper part of the figure depicts the event as it might appear on a scanning table, while the lower part gives SIMULATE's conception of it. The level number of a particle signifies the number of vertices plus one, that it takes to reach a particle in this diagram. Particle (3,1) represents the initial state consisting of particle (1,1), the incoming K^+ meson and particle (2,1), the target proton. Particle (3,1) has the total momentum of the initial state, which is the beam momentum and the energy of the initial state, which is the energy of the beam particle plus the target proton mass. [In the terminology of the program the notation (1,1) etc. refers to a particular particle at a particular level. That is, the first 1 in parentheses means particle number 1 and the second 1 refers to level 1.] Particle (3,1) then "decays" into two particles (1,2) and (2,2). Note that (3,1) was defined in such a way as to make its "decay" equivalent to the production of (1,2) and (2,2) by the initial system, beam plus target. Particles (1,2) and (2,2) decay into four particles, (1,3) (2,3), (3,3), and (4,3). These are the four final-state particles K^+, π^-, π^+, and p. The masses of these particles as well as the masses of the beam and target and the beam momentum are read in by SIMULATE as data. We note that the intermediate particles (1,2) and (2,2) are really composites, representing the $K^+\pi^-$ and $p\pi^+$ systems. The masses of these systems are not constant but are chosen by SIMULATE according to distributions which pertain to a particular process. Once both masses are chosen, the kinematics of a four-prong event are determined.

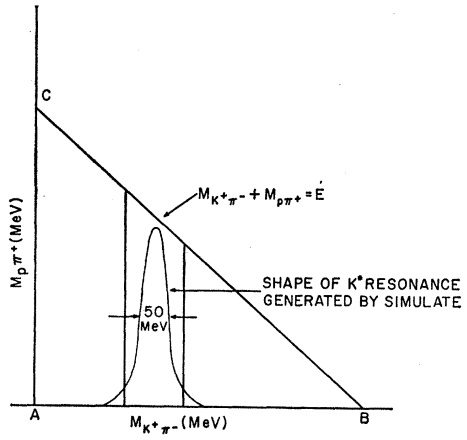

FIG. 10. Kinematic triangle for the reaction $K^+p \rightarrow K^+\pi^-\pi^+p$ (2.26 BeV/c). E=over-all c.m. energy=2338 MeV.

The method of selection of these masses may be described with the help of Fig. 10, which is a schematic drawing of the kinematic triangle for the reaction $K^+p \rightarrow K^+p\pi^+\pi^-$. The abscissa is the $K^+\pi^-$ effective mass and the ordinate, the $p\pi^+$ effective mass. An event which conserves energy can always be represented by a point in the triangle. As an example, we consider the generation of Lorentz-invariant phase-space events. As a first step, let us populate the triangle uniformly. SIMULATE first chooses a $K^+\pi^-$ mass randomly along line AB. It then chooses a $p\pi^+$ mass randomly along AC. Finally, it checks to see if its choice of masses is consistent with conservation of energy. If E is the total center-of-mass energy available, one must have

$$M_{K^+\pi^-}+M_{p\pi} \leq E. \tag{3}$$

If SIMULATE finds that this inequality is not satisfied it cycles back and chooses another pair of masses and again checks energy conservation. It does not proceed further until a pair of masses is found which lie inside the triangle. In making the random selection of masses (as well as angles—to be discussed shortly) SIMULATE uses a random number generator developed at the Johns Hopkins Applied Physics Laboratory for the IBM 7094. It generates random numbers uniformly over the interval 0 to 1. Thus if n is a number between 0 and 1, the probability that a number less than or equal to n will be generated equals n. The generator is used in the same way as a function subroutine. The name of the function is RRN and its initial argument determines a particular set of random numbers. Subsequent calls are always made to RRN(0). Thus, if we desire to set a variable X equal to a random number between 0 and 1 we write a FORTRAN statement:

$$X=\text{RRN}(0). \tag{4}$$

In choosing a mass uniformly and randomly along AB of Fig. 10, we would have

$$M_{K^+\pi^-}=M_A+\text{RRN}(0)(M_B-M_A). \tag{5}$$

By this process SIMULATE can generate as many pairs of masses as desired. If they are chosen uniformly along the $K^+\pi^-$ and $p\pi^+$ axes they will populate the triangle uniformly.

If we desire instead to generate K^* resonance events, rather than populating the entire triangle uniformly, we ask SIMULATE to choose $K^+\pi^-$ masses randomly according to a Gaussian distribution whose standard derivation is set equal to the half-width of the K^*. Thus we have, for example,

$$M_{K^+\pi^-} = M_{K^*} \pm \tfrac{1}{2}\Gamma_{K^*}(T), \tag{6}$$

where M_{K^*} is the central mass of the K^* and Γ_{K^*} is its full width at half-maximum. The variable T specifies the distance of the particular $K^+\pi^-$ mass from the central K^* mass. To obtain some value of T we first divide the area under the Gaussian function $y=(2\pi)^{-1/2}e^{-t^2/2}$ into 100 equal parts. This defines the values of a 100-element array in SIMULATE such that the nth element contains a subdivision point t_n, where t_n satisfies

$$\frac{1}{\sqrt{(2\pi)}}\int_0^{t_n} e^{-t^2/2}dt \Big/ \frac{1}{\sqrt{(2\pi)}}\int_0^{\infty} e^{-t^2/2}dt = \frac{n}{100}. \tag{7}$$

We then obtain a random number which we multiply by one hundred, obtaining a number m which lies between zero and one hundred. T is then set equal to t_m. If m is not an integer, the value of T is found by a linear interpolation between t_m and t_{m+1}. Finally, the choice of sign in (6) is determined by another random number which we truncate to an integer. If the integer is odd, the minus sign is chosen, if even, the plus sign.

To complete the mass selection for an event in which a K^* is produced along with an uncorrelated proton and pion, the $p\pi^+$ mass is chosen uniformly between its phase-space limits. As before, an energy check is made to ensure that the pair of masses chosen lies inside the triangle.

The generation of process "c" events described immediately above will populate only a portion of the kinematic triangle of Fig. 10. This will consist of a vertical band whose shape is Gaussian relative to the $M_{K^+\pi^-}$ axis. Within this band, events will be uniformly distributed along the $M_{p\pi^+}$ axis. In the same way SIMULATE can generate events in which the $p\pi^+$ mass is distributed according to a Gaussian whose maximum value occurs at the experimental value of the N^* mass and whose standard deviation is the N^* half-width. Finally, SIMULATE can choose both pairs of intermediate masses according to Gaussians, thus generating a set of double resonance, or process (b) events.

After having chosen a pair of intermediate masses for particles (1,2) and (2,2) SIMULATE proceeds to choose pairs of angles. At each vertex a reference frame and a set of coordinate axes are specified. Relative to these a pair of spherial angles (θ,ϕ) is chosen for each particle. Figure 9 shows that there are three vertices for a four-particle event. At each vertex, two pairs of angles corresponding to two outgoing particles must be selected, a total of 12 different angles. These angles are chosen according to experimental distributions by a random process in exactly the same manner as masses are chosen from a Gaussian distribution. SIMULATE uses several 100-element arrays for angular distributions. They are called TH1, TH2, TH3$\cdots$. They are read in as data. Thus TH1 contains a table of integrals of the distribution function for the production angle of particle (1,2). Suppose this angle for a particular process is distributed according to a function $f(\cos\theta)$. Then the nth element of TH1 is that value of $\cos\theta$ such that the integral of $f(\cos\theta)$ from zero to $\cos\theta$ is n hundredths of the integral from 0 to 1. In other words:

$$\text{TH1}(n) = \cos\theta_n,$$

with $\cos\theta_n$ satisfying

$$\int_0^{\cos\theta_n} f(\cos\theta)d(\cos\theta) \Big/ \int_0^{1} f(\cos\theta)d(\cos\theta) = \frac{n}{100}. \tag{8}$$

An angle is chosen by SIMULATE from this array with the help of an interpolation subroutine in a fashion similar to that explained above in connection with the choice of a mass.

We emphasize that all the distributions from which SIMULATE chooses variables are obtained from experimental data and that each process is done separately. Thus in the double-resonance process, the effective masses of particles (1,2) and (2,2) are chosen according to Gaussians with central values and widths appropriate for the K^* and N^*. The experimental production angular distribution of these particles is employed at the first vertex and the corresponding experimental K^* and N^* decay angular distributions at the second and third. Likewise for a single-resonance process in which say, a K^* alone is produced, we obtain form the experiment not only the K^* mass and angular distributions but also those of the proton-pion system which is produced along with the K^*.

The reference frames and coordinate axes relative to which all angles are chosen will now be described. At each vertex, the reference frame employed is the rest frame of the parent, or incoming particle. Thus, the angles for particles (1,2) and (2,2) are chosen in the rest frame of particle (3,1). Those for particles (1,3) and (2,3) are chosen in the rest frame of (2,2) and those for (3,3) and (4,3), in the rest frame of (1,2). The coordinate axes relative to which the angles are chosen are set up as follows: The z axis lies along the direction in which the parent particle is moving in the laboratory system; the x axis is normal to the plane of the interaction and the y axis is the cross product of z with x. Figure 11 shows the coordinate axes and angles for vertex 2 of Fig. 9 at which particle (2,2) decays into (1,3) and (2,3). The laboratory coordinate axes relative to which all three-momentum vectors are ultimately measured are

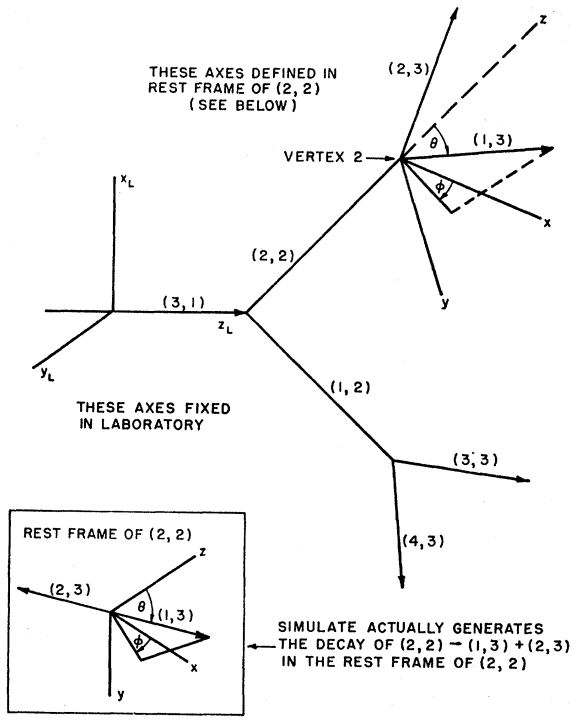

FIG. 11. Coordinate axes used in SIMULATE.

fixed in space, such that the laboratory z axis is along the beam direction or the direction of particle (3,1). These laboratory axes are shown in Fig. 11. We note also that since the decay at each vertex occurs in the rest frame of the decaying particle or parent, the two daughter particles must travel antiparallel to one another and therefore the angles chosen by SIMULATE for one decay particle automatically specify those for its partner. Thus in the decay of (2,2) into (1,3) and (2,3), a pair of angles $(\cos\theta,\phi)$ is chosen randomly from a specified distribution for (2,3) and those for (1,3) are then

$$\cos\theta(1,3) = -\cos\theta(2,3)\,, \tag{9}$$

$$\phi(1,3) = \phi(2,3) + \pi\,. \tag{10}$$

We now discuss the way in which the randomly selected kinematic variables are put together to produce an event, that is a set of four three-momentum vectors for the final particles (1,3), (2,3), (3,3), and (4,3). Output from SIMULATE consists of three direction cosines for each final-particle three-momentum and the magnitude of this three-momentum, all specified relative to the laboratory system of coordinate axes. We suppose that the variable selection has been completed. Then SIMULATE has in storage two intermediate masses [those of particles (1,2) and (2,2)] and 12 angles, two for each of the six particles (1,2), (2,2), and (1,3)–(4,3). One vertex is handled at a time. At each vertex the decay-particles' energy and momentum components are calculated in their center-of-mass system. Also a β and γ are calculated to be used in Lorentz transforming these quantities back to the laboratory system. The γ and β are usual relativistic quantities: $\beta = P/E$ and $\gamma = 1/(1-\beta^2)^{1/2}$, where P and E are the magnitude of three-momentum and energy of the parent particle relative to the laboratory system. At vertex 1 (Fig. 9), the total center-of-mass energy for decay into (1,2) and (2,2) is just the over-all center-of-mass energy of the reaction. At each of vertices 2 and 3, the total center-of-mass energy for decay is the corresponding intermediate mass (1,2) or (2,2). When the four-momenta of the decay particles and an appropriate γ and β have been calculated at a given vertex, control is turned over to a subroutine which uses the quantities calculated to transform the decay particles at that vertex back into the laboratory system. Finally we compute the direction cosines of these particles relative to the laboratory axes. For the intermediate particles, these direction cosines are necessary to specify the directions of the x, y, and z axes for decay into the final particles. Thus the laboratory direction cosines of (2,2) specify a direction which defines the z axis (and hence the x and y axes) for the decay of (2,2) into (1,3) and (2,3). The laboratory direction cosines plus the three-momenta of the final particles (1,3), (2,3), (3,3), and (4,3) are the final results of the generation.

We now return to discuss the problem of weighting events. We remark that SIMULATE does not keep every event it generates. Returning for a moment to the consideration of phase-space events, we point out that without a suitable weighting system a large number of generated phase-space events would populate the area of the kinematic triangle uniformly. In fact, even for a constant matrix element for the reaction the number of events having $K^+\pi^-$ mass between $M_{K^+\pi^-}$ and $M_{K^+\pi^-}+dM_{K^+\pi^-}$ and also $p\pi^+$ mass between $M_{p\pi^+}$ and $M_{p\pi^+}+dM_{p\pi^+}$ is not constant, but is proportional to[9]

$$R = P_1 \times P_2 \times P_3\,, \tag{11}$$

where P_i is the magnitude of the three-momentum of either decay particle at the ith vertex in the center-of-mass system at that vertex. Thus in order to obtain a sample of fictitious events which follow the predictions of Lorentz-invariant phase space, the uniformly populated kinematic triangle generated by SIMULATE must be depopulated in such a way that the number of events remaining in any small box of area of $dM_{K^+\pi^-} \times dM_{p\pi^+}$ is proportional to the right-hand side of (11). Actually this is done event by event without first generating all events. In other words, SIMULATE generates an event and decides whether to keep or reject it before the next event is generated. In carrying out the weighting procedure we first find by calculation, or by trial and error the maximum possible weight for our particular reaction. This number is read in by the program as data. Then

[9] G. Källén, *Elementary Particle Physics* (Addison-Wesley Publishing Corporation, Reading, Massachusetts, 1964).

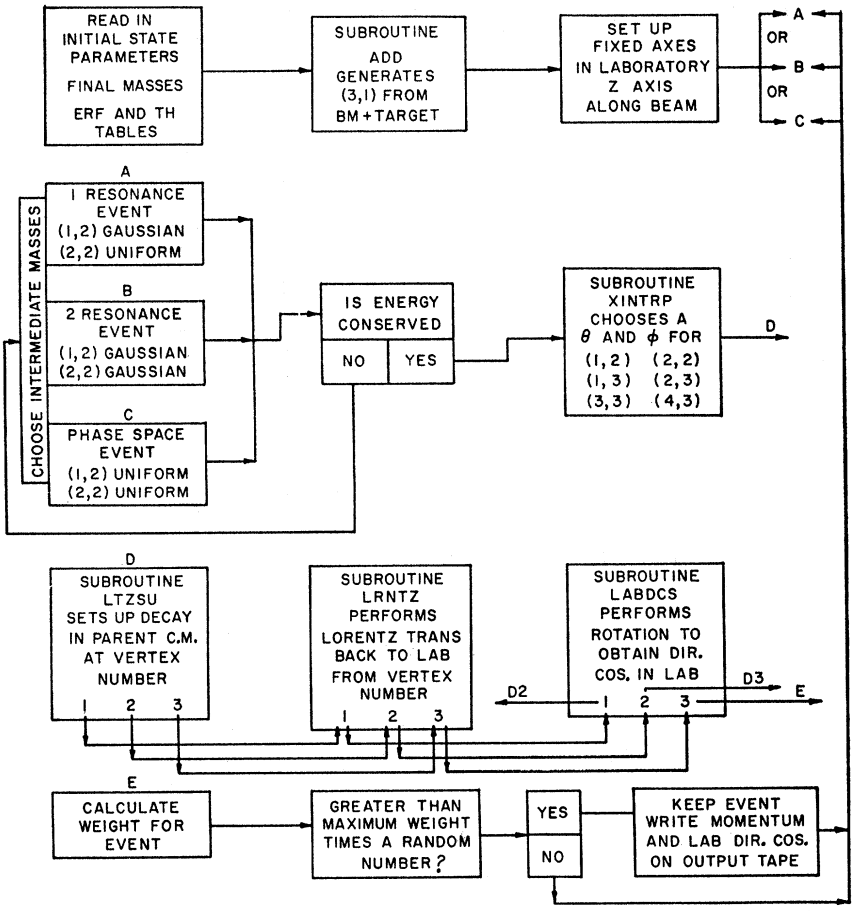

FIG. 12. Flow diagram of SIMULATE.

for each generated event SIMULATE obtains a weight according to Eq. (11). A random number is then obtarned which in turn is multiplied by the maximum weight. If the weight for the event is greater than the product of the random number and the maximum weight the event is kept—if not, it is rejected. In this way, the number of events remaining in any small region of the kinematic triangle is proportional to the value of R [Eq. (11)] corresponding to that region. Furthermore, all events, not only phase-space events may be treated in this way. For we have already weighted all resonance events according to a nonconstant matrix element by choosing the kinematic variables according to the proper mass and angular distributions. Hence in our model any further weighting will involve only the kinematic, or phase-space part of the amplitude. This has the advantage of saving computer time and of making the weighting procedure identical for all types of events. We present in Fig. 12 a flow diagram of SIMULATE which summarizes briefly the remarks made above concerning its operation.

The Monte Carlo Program SIMULATE is utilized in this experiment to generate a number of four-particle final-state events equal to the number of experimental events in this state. It is necessary to decide how many events in the experimental sample are appropriate to each of the four processes (a) through (d). We find that of the entire sample of 1296 experimental events, 148 events lie inside the kinematic triangle but outside both resonance bands. We assume that these 148 events are phase-space events. We then use SIMULATE to generate a large number of phase-space events and calculate the effective $K^+\pi^-$ and $p\pi^+$ masses. We proceed then to plot these mass pairs in a kinematic triangle until we have 148 events outside the resonance bands. We assume that all fictitious events plotted up to that point give a good estimate of the total number of phase-space events in the experiment. We find that 350 events are required to produce 148 events outside the resonance bands. By subtracting the numbers of phase-space events lying in each of the bands on the simulated plot ($350-148=202$ events) from the bands in the experimental plot we obtain an estimate of the fractions of the experimental events which proceeded according to one or another of the resonance amplitudes. According to this analysis we estimate that the reaction $K^+p \to K^+p\pi^+\pi^-$

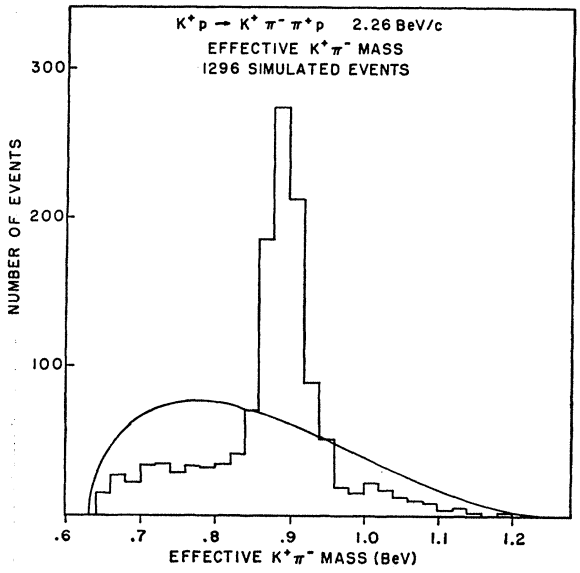

FIG. 13. Effective $K^+\pi^-$ mass for fake events.

at 2.26 BeV/c proceeds by way of four amplitudes as follows:

(a) $K^+p \to K^+\pi^-\pi^+p$, $27\pm5\%$,
(b) $K^+p \to K^*N^* \to K^+\pi^-\pi^+p$, $48\pm5\%$,
(c) $K^+p \to K^*p\pi^+ \to K^+\pi^-\pi^+p$, $10\pm5\%$,
(d) $K^+p \to K^+\pi^-N^* \to K^+\pi^-\pi^+p$, $15\pm5\%$.

Thus, we use SIMULATE to generate 1296 fictitious events 27% of which are process (a) events, 48% of which are

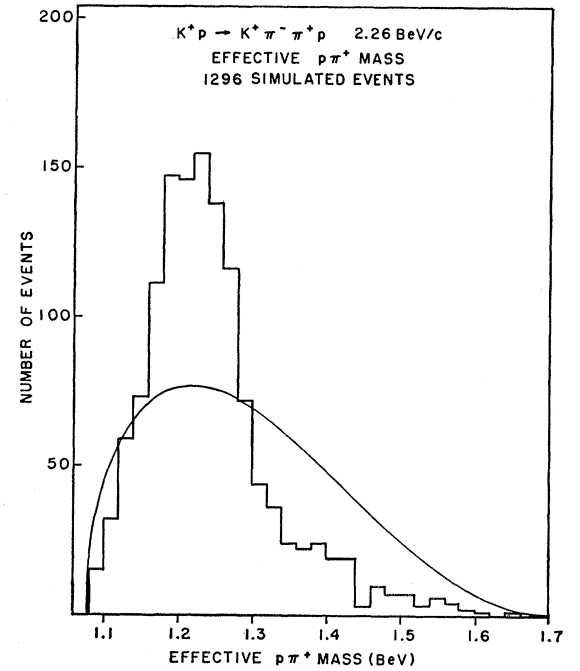

FIG. 14. Effective $p\pi^+$ mass for fake events.

(b) events, and so on. Table III is a list of all input information supplied to SIMULATE. We emphasize strongly that this information is obtained entirely from the experiment. The vertices and particle numbers referred to in the table are shown in Fig. 9. At each vertex only one pair of decay angles need be specified since all decays

TABLE III. SIMULATE input information.

	A: Phase-space events
Vertex 1:	
(1,2) mass dist.	Constant between 1078–1704 MeV
(2,2) mass dist.	Constant between 634–1260 MeV
$\cos\theta(2,2)$ dist.	Constant
$\varphi(2,2)$ dist.	Constant
Vertex 2:	
$\cos\theta(2,3)$ dist.	Constant
$\varphi(2,3)$ dist.	Constant
Vertex 3:	
$\cos\theta(4,3)$ dist.	Constant
$\varphi(4,3)$ dist.	Constant
	B: Double-resonance events
Vertex 1:	
(1,2) mass dist.	Gaussian, $M_0=1210$ MeV, $\Gamma=120$ MeV
(2,2) mass dist.	Gaussian, $M_0=895$ MeV, $\Gamma=50$ MeV
$\cos\theta(2,2)$ dist.	Constant $\cos\theta<0$; $1-13\cos\theta+32\cos^2\theta$ $\cos\theta\geqslant 0$
$\varphi(2,2)$ dist.	Constant
Vertex 2:	
$\cos\theta(2,3)$ dist.	$1+1.4\cos^2\theta$
$\varphi(2,3)$ dist.	Constant
Vertex 3:	
$\cos\theta(4,3)$ dist.	$1-0.43\cos\theta+0.40\cos^2\theta$
$\varphi(4,3)$ dist.	Constant
	C: K^* single-resonance events
Vertex 1:	
(1,2) mass dist.	Gaussian, $M_0=895$ MeV, $\Gamma=50$ MeV
(2,2) mass dist.	Uniform between 1078–1704 MeV
$\cos\theta(2,2)$ dist.	Constant $\cos\theta>0$; $1+2.6\cos\theta+10\cos^2\theta$ $\cos\theta\leqslant 0$
$\varphi(2,2)$ dist.	Constant
Vertex 2:	
$\cos\theta(2,3)$ dist.	$1+\cos\theta+\cos^2\theta$
$\varphi(2,3)$ dist.	Constant
Vertex 3:	
$\cos\theta(4,3)$ dist.	$1+0.5\cos\theta+1.5\cos^2\theta$
$\varphi(4,3)$ dist.	Constant
	D: N^* single-resonance events
Vertex 1:	
(1,2) mass dist.	Gaussian $M_0=1210$ MeV, $\Gamma=120$ MeV
(2,2) mass dist.	Uniform between 634–1260 MeV
$\cos\theta(2,2)$ dist.	Constant $\cos\theta<0$; $1-4.5\cos\theta+13.5\cos^2\theta$ $\cos\theta\geqslant 0$
$\varphi(2,2)$ dist.	Constant
Vertex 2:	
$\cos\theta(2,3)$ dist.	$1+\cos^2\theta$
$\varphi(2,3)$ dist.	Constant
Vertex 3:	
$\cos\theta(4,3)$ dist.	$1-\cos\theta+\cos^2\theta$
$\varphi(4,3)$ dist.	Constant

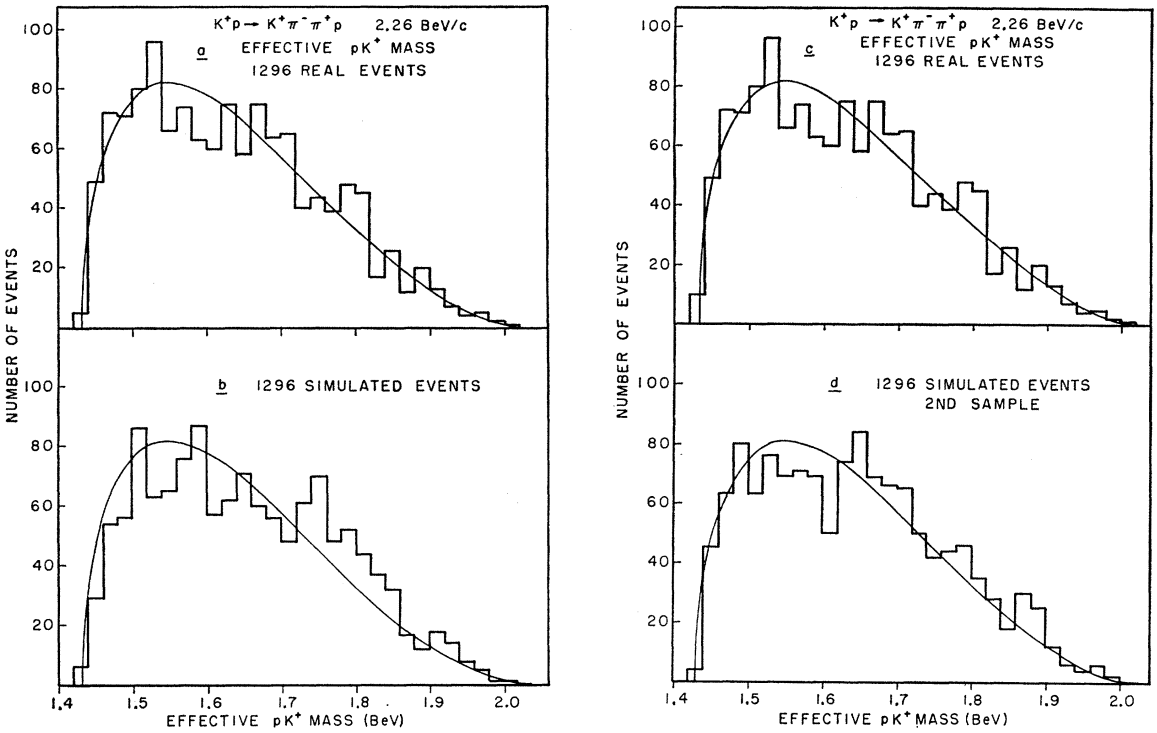

FIG. 15. Effective pK^+ mass for real events and two samples of fake events.

take place in the center-of-mass system of the decaying particles.

6. RESULTS OF MONTE CARLO CALCULATION

Figures 13 through 24 display the results of the Monte Carlo calculation. Most of these figures have two sections (a) and (b). In each case, the (a) section is a histogram of the effective mass of some combination of particles taken from the experiment. These are labeled real

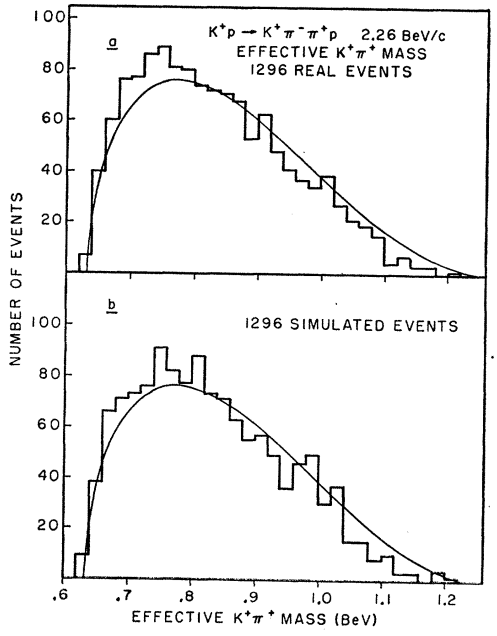

FIG. 16. Effective $K^+\pi^+$ mass for real and fake events.

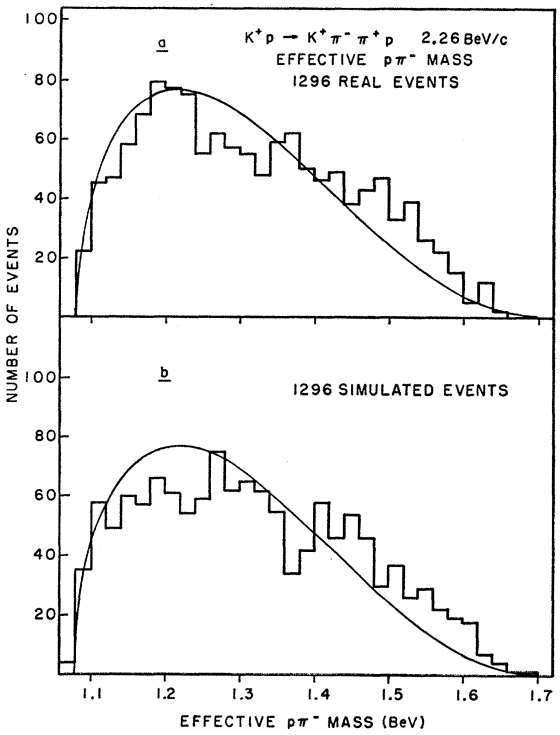

FIG. 17. Effective $p\pi^-$ mass for real and fake events.

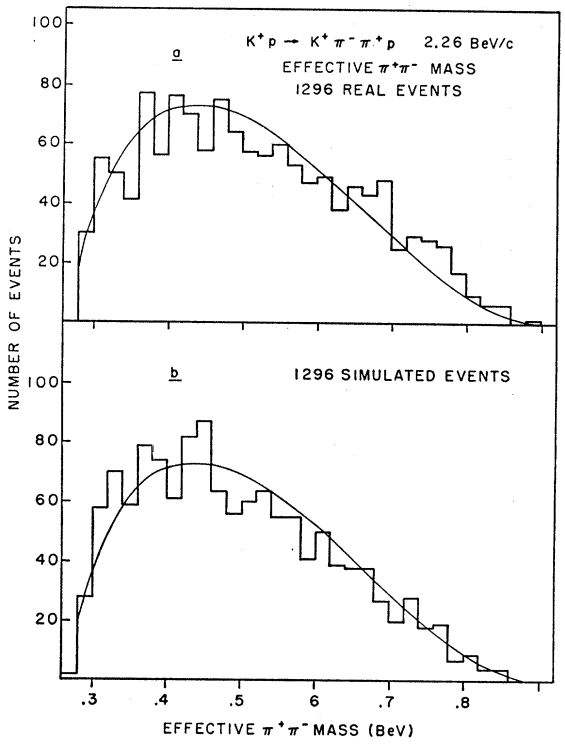

FIG. 18. Effective $\pi^+\pi^-$ mass for real and fake events.

events. The (b) section is the corresponding effective-mass histogram for simulated events. The appropriate Lorentz-invariant phase-space curves, normalized to the total number of events are included in these figures. To check the validity of the calculation, we generate a second independent set of fictitious events with exactly the same input quantities as the first. The independence of the two sets is accomplished by using different sequences of random numbers.

Figures 13 and 14 show, respectively, the $K^+\pi^-$ and $p\pi^+$ mass distributions for the fictitious events. These are in a sense controls for the remainder of the results because they represent input to the Monte Carlo program. The strong K^* and N^* signals are observed and these plots should be compared with the experimental $K^+\pi^-$ and $p\pi^+$ mass distributions (Figs. 2 and 3). Figures 15(a) and (b) is a comparison of the pK^+ mass distributions from experimental and simulated data. The deviations from Lorentz-invariant phase space in the experimental distribution are small. The simulated events, however, show an excess above phase space from 1720 to 1860 MeV. To check this, the pK^+ mass spectrum for the second independent sample of simulated events is shown in Figs. 15(c) and (d). The excess does not appear here. The difference between the two simulated histograms is a measure of the statistical variations we may expect in our Monte Carlo events. Figure 16 is the effective-mass distribution of the $K^+\pi^+$ system. The agreement between the real and fictitious events here is very good. Except for small excess between 660 and 800 MeV both distributions agree very well with the predictions of phase space. Apparently the N^* and K^* production does not appreciably affect the $K^+\pi^+$ mass

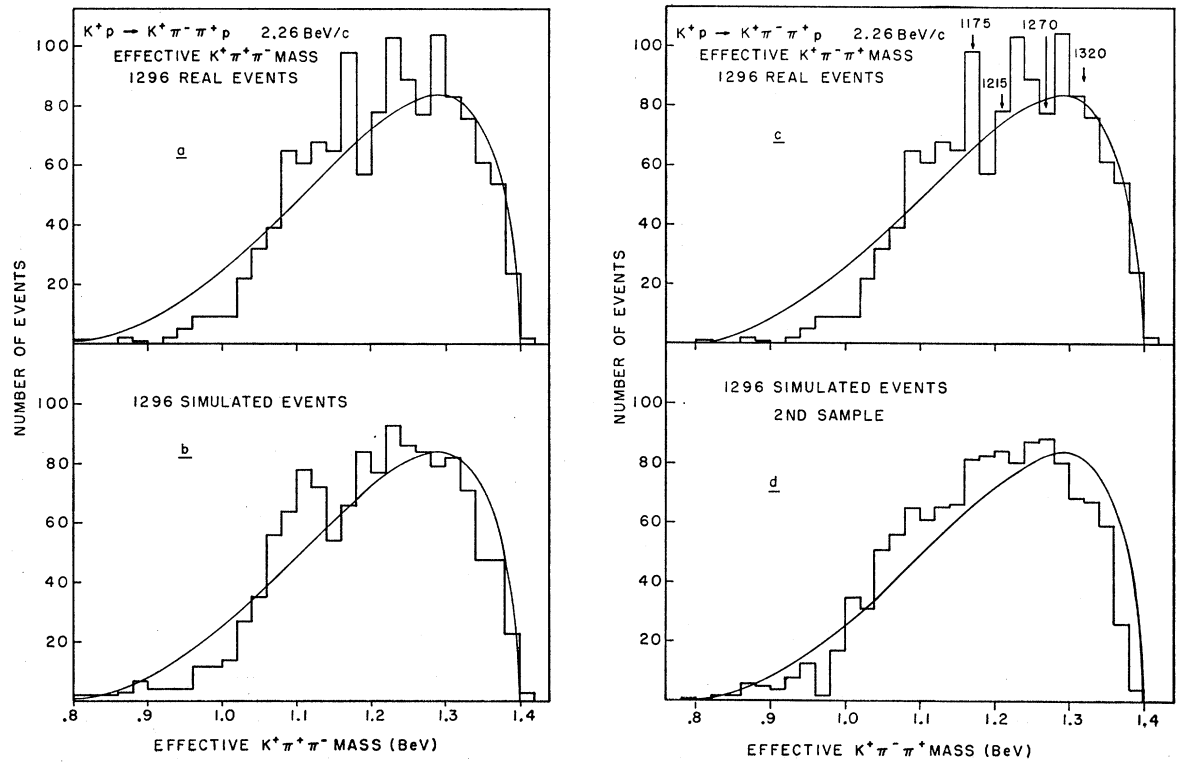

FIG. 19. Effective $K^+\pi^+\pi^-$ mass for real events and two samples of fake events.

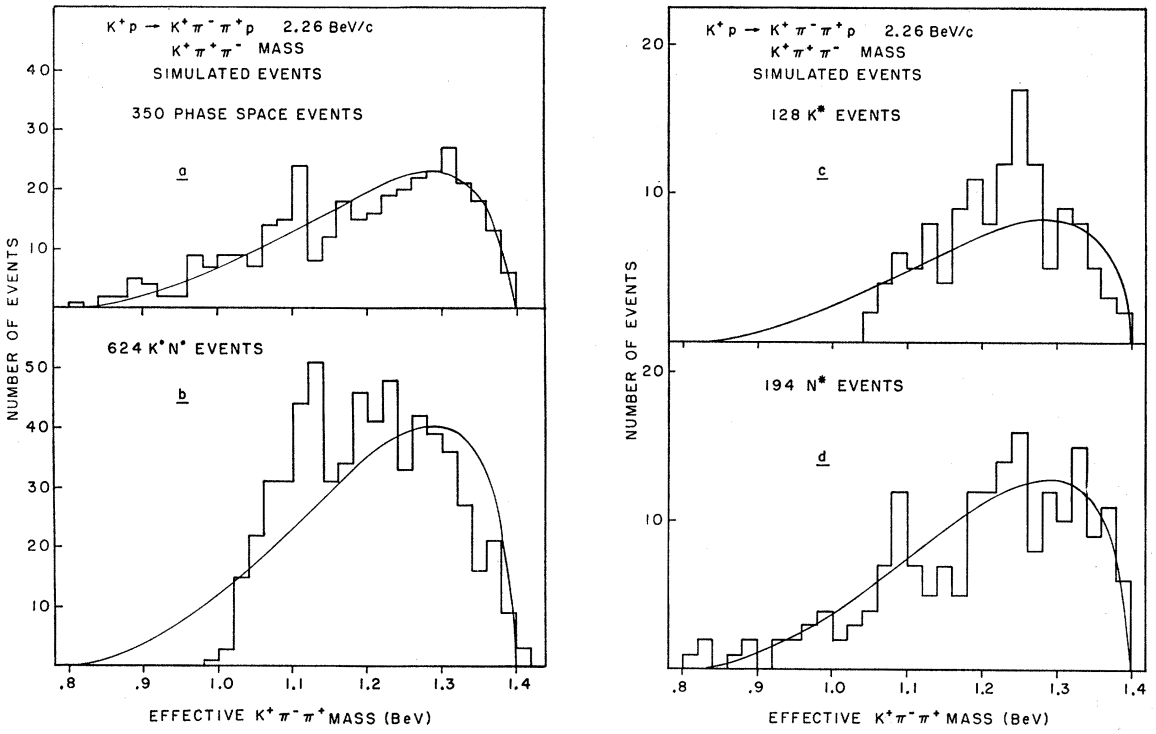

FIG. 20. Effective $K^+\pi^+\pi^-$ mass from four different simulated processes.

spectrum. We note in passing that there is no evidence in our data for the production of an isospin-$\frac{3}{2}$ state in the $K^+\pi^+$ system. Figure 17 shows the mass distributions for the $p\pi^-$ system. The simulated events show an apparent depletion relative to the real events in the mass region 1140–1260 MeV. The reason for the disparity is possibly a weak $N^*(1238)$ signal in the experiment. The model used to generate the fake events did not include this possibility. Therefore, we should not expect to see a corresponding $N^*(1238)$ peak in the fake events. Figure 18 is a plot of the $\pi^+\pi^-$ mass distribution for real and fake events. The experimental and Monte Carlo distributions agree very well and both seem to be well approximated by Lorentz-invariant phase space.

We now turn to three-particle mass combinations. We plot the effective mass of the $K^+\pi^+\pi^-$ system in Fig. 19. Several groups have reported enhancements in $K\pi\pi$ mass distributions—Wangler *et al.*[10] observed such an enhancement at 1175 MeV in π^-p collisions at 3.0 BeV/c in the final states $\Lambda^0K^+\pi^-\pi^0$, $\Lambda^0K^0\pi^+\pi^-$, $\Sigma^0K^0\pi^+\pi^-$, and $\Sigma^-\pi^+K^0\pi^0$. This was verified by Miller *et al.*[11] and more recently Bishop *et al.*[12] have reported a $K^0\pi^+\pi^+$ enhancement in the reaction $K^+p \to K^0\pi^+\pi^+p\pi^-$. In the present experiment an excess is observed between 1080 and 1180 MeV. However, both samples of simulated events also show this excess [Figs. 19(b) and (d)]. Quantitatively we take 1170 MeV as a central mass and 60 MeV as a width for a possible $K\pi\pi$ state in this region

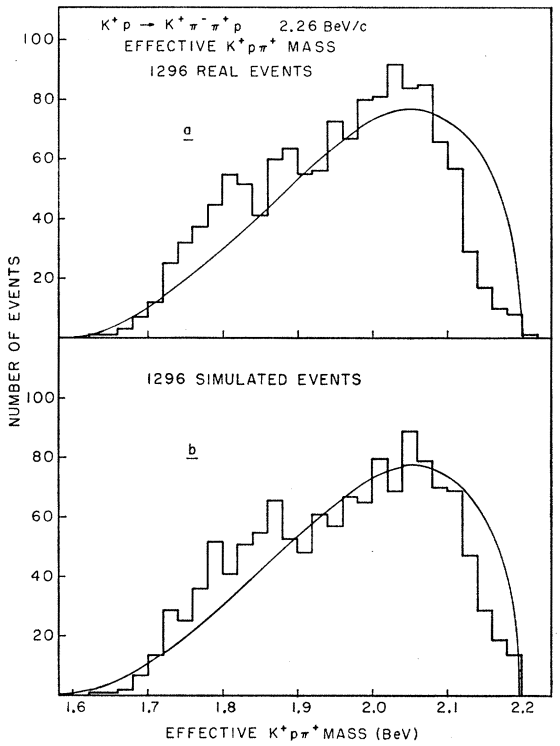

FIG. 21. Effective $K^+p\pi^+$ mass for real and fake events.

[10] T. P. Wangler, A. R. Erwin, and W. D. Walker, Phys. Letters 9, 71 (1964).
[11] D. H. Miller, A. Z. Kovacs, R. L. McIlwain, T. R. Palfrey, and G. W. Tautfest, Phys. Letters **15**, 74 (1965).
[12] J. M. Bishop, A. T. Goshaw, A. R. Erwin, M. A. Thompson, W. D. Walker, and A. Weinberg, Phys. Rev. Letters **16**, 1069 (1966).

and consider the interval 1140 MeV$\leqslant M_{K\pi\pi}\leqslant$1200 MeV. We find 220 experimental events in this interval. Using the two samples of fictitious events as the correct "phase space" with which to compare the experimental plot, we find, respectively, 204 and 229 events in this same interval. This represents a one-standard-deviation enhancement relative to the first fictitious sample and no enhancement relative to the second. We conclude that there is no evidence for a $K\pi\pi$ resonance at 1170 MeV in our data. A $K\pi\pi$ enhancement at 1215 MeV has been reported by a Columbia-Rutgers group[13] and a CERN group.[14] The reactions were $p\bar{p}$ annihilations at rest: $p\bar{p}\rightarrow K\bar{K}\pi\pi$ with at least one neutral K meson decaying by a two-pion mode. Furthermore, a CERN group[15] has also reported a 1270-MeV enhancement in $K\pi\pi$ spectra from the reaction $p\bar{p}\rightarrow K^0K^{\pm}\pi^{\mp}\pi^+\pi^-\pi^0$. In the present experiment a small enhancement above ordinary phase space is observed in the region 1200–1260 MeV [Figs. 19(a) and (c)]. This might possibly be related to one or the other of the excesses at 1215 or 1270 MeV. However, the simulated events also show these excesses relative to ordinary Lorentz-invariant phase space in this region. The number of experimental events between 1200–1260 MeV is 270. Using the simulated sample of events in Fig. 19(b) as the "correct" phase space for comparison we find 256 events in this interval. The 1200–1260 excess is therefore less than one standard deviation. If we use the second fictitious sample as phase space we find 251 events in this range giving an experimental excess of about one standard deviation. Thus our excess in the 1200–1260-MeV region of the $K\pi\pi$ mass spectrum does not appear to be significant. In a K^+p experiment at CERN[16] at 5.0 BeV/c a 100-MeV wide enhancement was reported at 1320 MeV in the $K\pi\pi$ spectrum from the reaction $K^+p\rightarrow K^+\pi^-\pi^+p$. No evidence for this is observed in the present experiment [Figs. 19(a), (b), (c), and (d)]. It is of some interest to separate the Monte Carlo events into four distinct processes and plot the contribution of each to the $K^+\pi^+\pi^-$ mass spectrum. This is done in Figs. 20(a), (b), (c), and (d). Figure 20(a) is the $K\pi\pi$ mass distribution for events generated according to a constant matrix element. Figure 20(b) is the $K\pi\pi$ distribution for events generated according to the K^*-N^* or double-resonance process. This plot is rather drastically distorted relative to ordinary phase space and in particular, the effect between 1200 and 1260 MeV discussed above is seen to originate partly from this group of events. The events in which only a K^* was generated are shown in Fig. 20(c). The 1200–1260 excess is plainly visible here also. Events in which only an N^* was generated are shown in Fig. 20(d). From these plots we conclude that the departure from ordinary Lorentz-invariant phase space which are observed in the $K\pi\pi$ mass spectrum derive mainly from configurations in which the $K^+\pi^-$ system resonances as a K^*. We remark finally, in connection with the $K\pi\pi$ mass spectrum that we are just below threshold for the production of the $K^*(1400)$.[17]

The $K^+p\pi^+$ mass distribution is shown in Fig. 21. Various small excesses along the upward slope of the ordinary phase-space curve are present in this spectrum. The simulated events agree quite well with the real

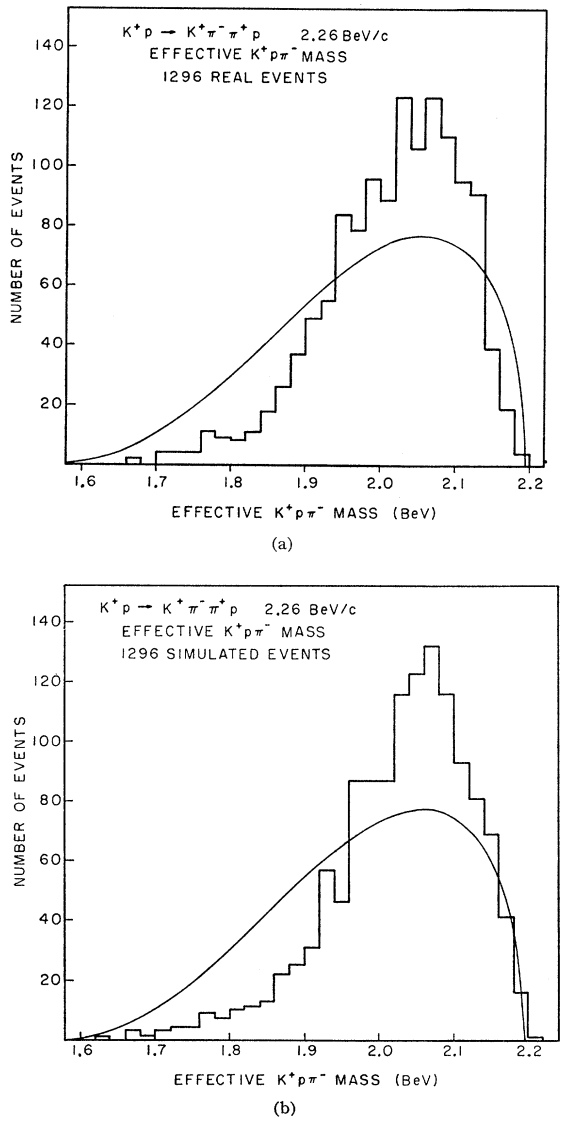

FIG. 22. Effective $K^+p\pi^-$ mass for real and fake events.

[13] N. Barash, J. Steinberger, T. H. Tau, L. Kirsch, P. Franzini, report presented at The 1964 International Conference on High Energy Physics at Dubna.

[14] R. Armenteros, P. N. Edwards, T. Jacobsen, L. Montonet, A. Shapira, J. Vandermeulen, Ch. D'Audlou, A. Ostier, P. Baillon, J. Cohen-Gousuna, C. Defoix, J. Siaud, C. Glesquiere, and P. Rivet, Phys. Letters **9**, 207 (1964).

[15] B. R. French, J. B. Vinson, V. Simak, J. Badier, M. Bazin, A. Monge, P. Grieve, report presented at The 1964 International Conference on High Energy Physcis at Dubna.

[16] S. P. Almeidee, H. W. Atherton, T. A. Byer, P. J. Dorman, A. G. Forson, J. H. Scharenquivel, D. M. Sendall, and B. A. Westwood, Phys. Letters. **16**, 184 (1965).

[17] N. Haque *et al.*, Phys. Letters **14**, 338 (1965).

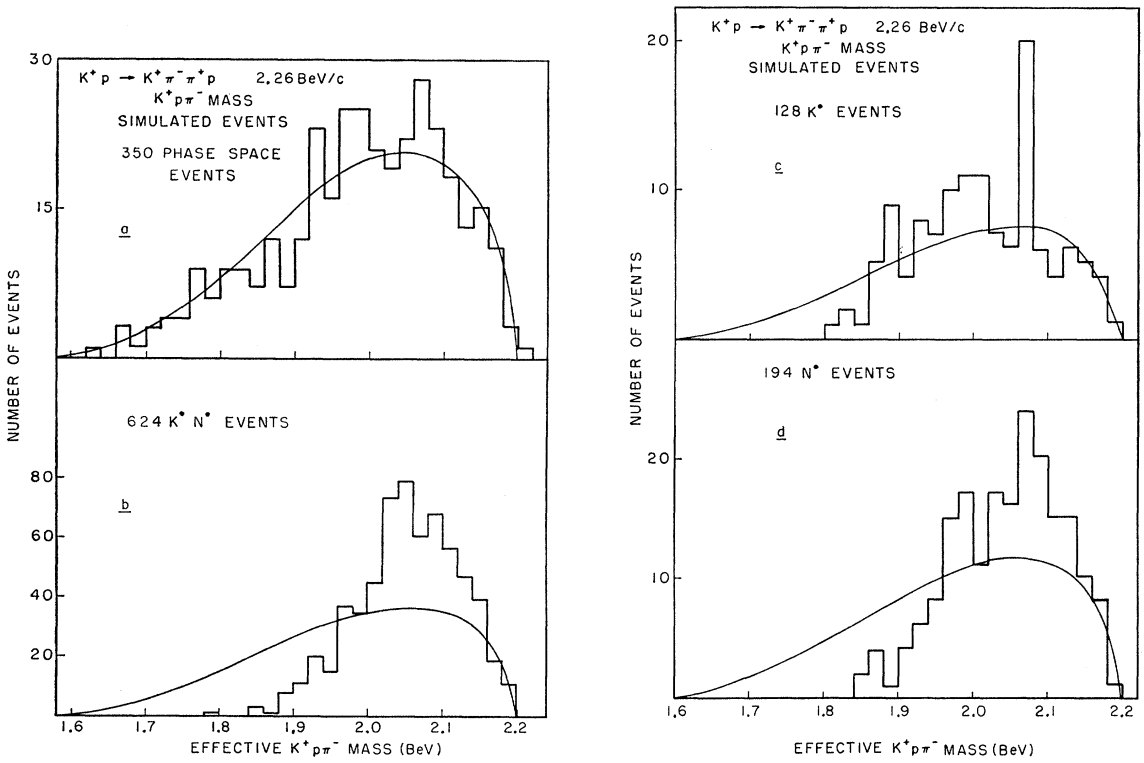

FIG. 23. Effective $K^+p\pi^-$ mass from four different simulated processes.

events. We discuss now the $K^+p\pi^-$ mass distribution. A very strong enhancement about 200 MeV wide is observed centered about a mass of 2040 MeV [Fig. 22(a)]. Relative to ordinary phase space this is a nine-standard-deviation effect. Figure 22(b), which is the corresponding mass distribution for the fictitious events shows that this effect is only a reflection. To investigate its origin the $K^+p\pi^-$ mass spectrum is plotted for the various in-

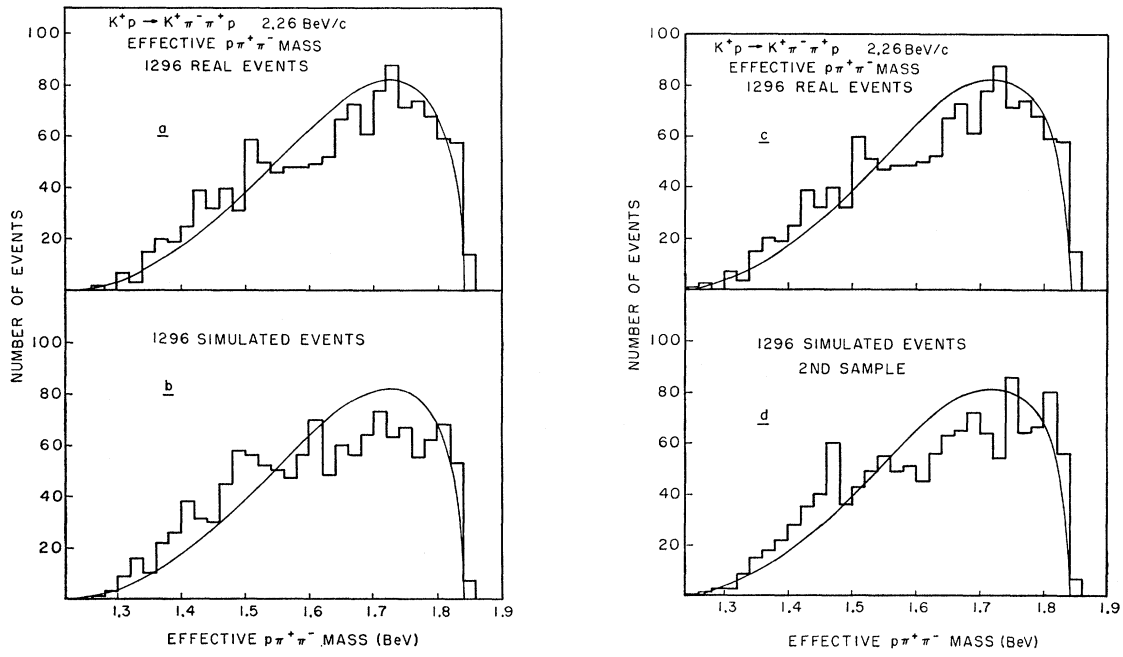

FIG. 24. Effective $p\pi^+\pi^-$ mass for real and fake events.

dividual processes in Figs. 23(a)–(d). The effect is apparently associated mostly with the N^* in the $p\pi^+$ system for it shows up strongly in the double resonance events and in the N^* only events.

The final spectrum to be discussed is that of the $p\pi\pi$ system (Fig. 24). Relative to the simulated events, the real events show an excess in the mass region between 1620 and 1840 MeV. Once again, we use the second sample of simulated events to determine whether the effect is statistically significant. Figures 24(c) and (d) show the real event and the second fictitious sample. In the interval 1620–1840 MeV the experimental distribution has 689 events. In this same region the fictitious distribution has 670 events. Therefore relative to the second sample of fake events as phase space for the reaction, the experimental excess is considerably less than one standard deviation.

We conclude from the foregoing that the data for the reaction $K^+p \to K^+\pi^-\pi^+p$ is consistent with a model in which four incoherent processes are assumed to occur with the relative rates indicated:

$$K^+p \to K^+p\pi^+\pi^-, \quad 27\pm5\%$$
$$K^+p \to K^*N^* \to K^+p\pi^+\pi^-, \quad 48\pm5\%$$
$$K^+p \to K^*p\pi^+ \to K^+p\pi^+\pi^-, \quad 10\pm5\%$$
$$K^+p \to K^+\pi^-N^* \to K^+p\pi^+\pi^-, \quad 15\pm5\%.$$

We remark that a weak neutral N^* may be present in the data, a possibility indicated by a slight disparity between the experimental $p\pi^-$ mass distribution and the corresponding distribution predicted by the model. Finally we have seen no evidence for the production of any resonance other than the $K^*(895)$ and $N^*(1238)$. In particular our $K\pi\pi$ mass distribution is not consistent with enhancements at 1170, 1215, 1270, or 1320 MeV.

7. A NOTE ON THE FIVE-PARTICLE EVENT $K^+p \to K^+p\pi^+\pi^-\pi^0$

We have also used our Monte-Carlo-generated events to aid in the analysis of our five-particle final-state events of the type $K^+p \to K^+p\pi^+\pi^-\pi^0$. A search for the κ(725 MeV) meson in this channel was initiated. We found nothing significant in any of the mass spectra except the $K^+\pi^0$ distribution which is shown in Fig. 25. A peak occurs at about 670 MeV whose width is 60 MeV. The effect amounts to about 3.5 standard deviation above Lorentz-invariant phase space.

The low mass of this peak makes it rather suspect. This suspicion increases when we discover that the laboratory momentum of the fitted π^0 in these events is invariably less than 100 MeV/c. We felt that this peak might therefore be a spurious effect, due possibly to four-particle events which were mistakenly fitted and then misidentified at the scan table as five-particle events. This is a reasonable guess, because the unfitted missing momentum from a sample of four-constraint four-

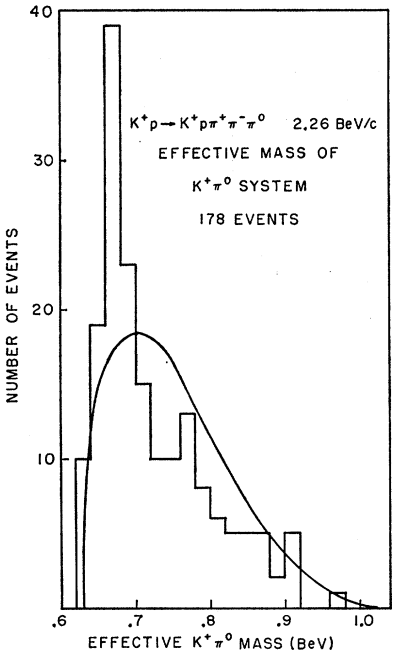

FIG. 25. Effective $K^+\pi^0$ mass from the reaction $K^+p \to K^+p\pi^+\pi^-\pi^0$.

particle events is found to be on the average, about 50 MeV/c. We therefore subtracted from the experimental sample of 178 five-particle events all those which had been fitted as four-constraint fits with a probability of greater than 1%. After the subtraction, 141 events remained. Their $K^+\pi^0$ mass distribution is shown in Figure 26. The peak has not disappeared.

To investigate this matter further we sent a sample of 500 fictitious four-particle Monte Carlo events through the fitting program KICK. These events were distributed according to the various experimental processes [(a)–(d)] discussed previously. Before entering the fitting program they were sent through a preliminary program which pulled the various kinematical quantities, like momentum and angles, off their exact values so as to render the Monte Carlo events identical to a sample of measured events. Also, this preliminary program assigned track lengths to the events and distributed them in the 20-in. bubble chamber using the real events as a guide.

The main results of sending these fake events through the fitting program are

(a) Only 20 failed to be fitted with the correct hypothesis with greater than 1% probability.

(b) There were 209 events (nearly half) which were fitted with a false neutral π. This agreed very well with a sample of 500 real four-constraint events ($K^+p \to K^+p\pi^+\pi^-$) for which, about one-half had a one constraint π^0 fit with greater than 1% probability.

(c) Of the 20 fake events which failed as four-constraint fits, only four were fitted as one-constraint fit with probability greater than 1%. This means that a real four-particle event will fail as such (probability less than

1%) but pass as a one-constraint five-particle event (greater than 1% probability) only in about 1% of the cases. Thus we are not nearly entitled to remove any more events from the plot in Fig. 26.

Despite the result mentioned in (c) above, we plotted the effective $K^+\pi^0$ mass for all fake-event fits which had a π^0. We did not attempt here to choose among multiple π^0 fits in a given event when there were more than one. We simply included all fits, so that in Fig. 27, which shows the distribution, some events are plotted more than once. We see from this figure that when a false neutral is added, the effective $K^+\pi^0$ mass is almost always less than 720 MeV.

We do not wish to draw any conclusions from the above. We simply note that the introduction of a false neutral particle often occurs in a fitting program and in these circumstances this neutral particle and one of the charged visible particles may simulate a peak in their effective mass distribution. We finally remark in connection with the five-body reaction $K^+p \to K^+p\pi^+\pi^-\pi^0$ that no enhancement at 730 MeV (corresponding to the κ meson) is observed in our data.

8. CONCLUSION

For the reaction $K^+p \to K^+p\pi^+\pi^-$ at 2.26 BeV/c we find a cross section of (1.7±0.2) mb and a partial cross section for $K^+p \to K^*N^* \to K^+p\pi^+\pi^-$ of (0.8±0.1) mb. The decay angular distributions of the K^* and N^* in the double-resonance process indicate on the whole, consistency with a single-pion-exchange model for their production. The data are in disagreement with the absolute cross section predicted for the reaction $K^+p \to K^*N^*$ by the model, but are in excellent agreement with the theoretical shape of the differential cross section.

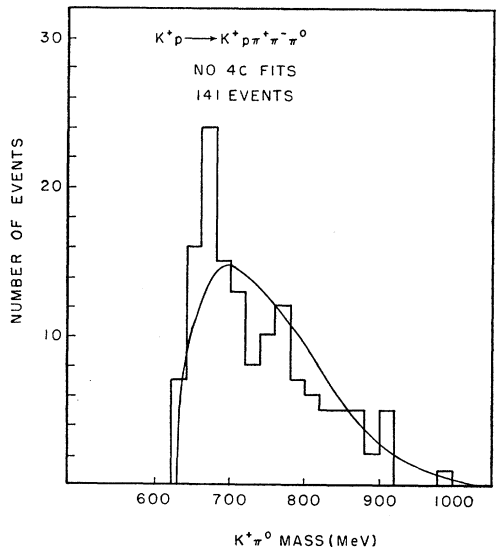

FIG. 26. Effective $K^+\pi^0$ mass from the reaction $K^+p \to K^+p\pi^+\pi^-\pi^0$ with all events having a possible 4-constraint fit removed.

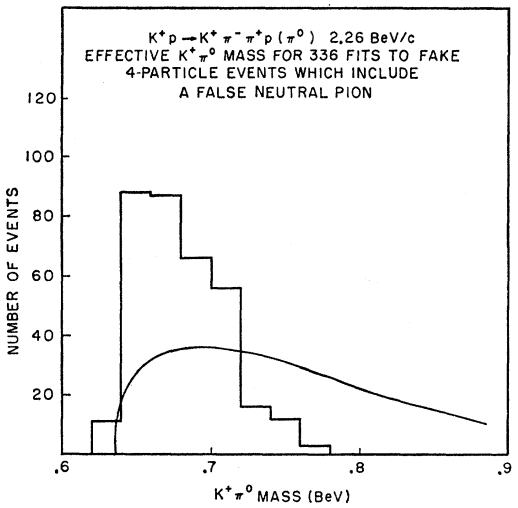

FIG. 27. $K^+\pi^0$ effective mass for all false neutral π fits.

A Monte Carlo analysis of the channel $K^+p \to K^+p\pi^+\pi^-$ indicates that our data are consistent with a model in which only the $K^*(895)$ and $N^*(1238)$ resonances are produced along with phase space.

Finally, we have seen no evidence for the production of the κ (730 MeV) in either the $K^+\pi^-$ or $K^+\pi^0$ mass spectra of the five-particle reaction $K^+p \to K^+p\pi^+\pi^-\pi^0$.

ACKNOWLEDGMENTS

We gratefully acknowledge the cooperation of the operating crew of the 20-in. hydrogen bubble chamber at Brookhaven. We would like to express our thanks to Dr. Gordon Kane for many helpful discussions of all aspects of this work, and to Dr. J. D. Jackson and his colleagues at the University of Illinois for calculating the theoretical cross sections predicted by the Peripheral Model. We appreciate the excellent work of the scanning and measuring staff at Johns Hopkins. We are very grateful to Mrs. Doris Ellis for the modification and execution of the many computer programs which were used in all phases of this work.